energies

MDPI

Article

Electricity Demand Forecasting and Risk Assessment for Campus Energy Management

Yon-Hon Tsai [1] and Ming-Tang Tsai [2,*]

[1] Institute of Mechatronics Engineering, Cheng-Shiu University, Kaohsiung 833, Taiwan; ybantw@gcloud.csu.edu.tw
[2] Department of Electrical Engineering, Cheng-Shiu University, Kaohsiung 833, Taiwan
* Correspondence: k0217@gcloud.csu.edu.tw; Tel.: +886-7-7310606

Abstract

This paper employs the Grey–Markov Model (GMM) to predict users' electricity demand and introduces the Enhanced Monte Carlo (EMC) method to assess the reliability of the prediction results. The GMM integrates the advantages of the Grey Model (GM) and the Markov Chain to enhance prediction accuracy, while the EMC combines the Monte Carlo simulation with a dual-variable approach to conduct a comprehensive risk assessment. This framework helps decision-makers better understand electricity demand patterns and effectively manage associated risks. A university campus in southern Taiwan is selected as the case study. Historical data of monthly maximum electricity demand, including peak, semi-peak, Saturday semi-peak, and off-peak periods, were collected and organized into a database using Excel. The GMM was applied to predict the monthly maximum electricity demand for the target year, and its prediction results were compared with those obtained from the GM and Grey Differential Equation (GDE) models. The results show that the average Mean Absolute Percentage Error (MAPE) values for the GM, GDE, and GMM are 10.96341%, 9.333164%, and 6.56026%, respectively. Among the three models, the GMM exhibits the lowest average MAPE, indicating superior prediction performance. The proposed GMM demonstrates robust predictive capability and significant practical value, offering a more effective forecasting tool than the GM and GDE models. Furthermore, the EMC method is utilized to evaluate the reliability of the risk assessment. The findings of this study provide decision-makers with a reliable reference for electricity demand forecasting and risk management, thereby supporting more effective contract capacity planning.

Keywords: Monte Carlo; grey model; risk assessment; electricity demand prediction

check for updates

Academic Editors: Wenxiao Chu and Chi-Chuan Wang

Received: 22 September 2025
Revised: 10 October 2025
Accepted: 16 October 2025
Published: 20 October 2025

Citation: Tsai, Y.-H.; Tsai, M.-T. Electricity Demand Forecasting and Risk Assessment for Campus Energy Management. *Energies* **2025**, *18*, 5521. https://doi.org/10.3390/en18205521

Copyright: © 2025 by the authors. Licensee MDPI, Basel, Switzerland. This article is an open access article distributed under the terms and conditions of the Creative Commons Attribution (CC BY) license (https://creativecommons.org/licenses/by/4.0/).

1. Introduction

With the expansion of educational resources and digital teaching in Taiwan, the demand for electricity on campuses has been increasing year by year. Electrical equipment is widely distributed across campuses, covering teaching, research, daily life, and other areas. As the number of student increases, the overall electricity consumption of campuses continues to grow. However, electricity management is often conducted independently by each department, lacking effective coordination and overall planning. A significant amount of investment is required in campus power infrastructure to consistently meet peak demand. Yet peak demand frequently exceeds the contracted capacity, increasing electricity costs. As a result, electricity prices rise, placing considerable burdens on the electricity expenditures of institutions. Therefore, effective power management technologies are

essential. Peak demand prediction plays a crucial role in power management strategies, as it helps accurately define the contracted capacity that should be adopted by campuses to reduce electricity costs. Thus, demand prediction has become one of the key elements in campus power management strategies [1–3].

In Taiwan, Taiwan Power Company (TaiPower, Taipei, Taiwan) is a monopoly power utility that sells electricity to consumers. The contract capacity of TaiPower is set based on the Time-of-Use (TOU) tariff system [4], which includes peak periods, semi-peak periods, Saturday semi-peak periods, and off-peak periods. The contracted capacity serves as the basis for calculating the basic electricity charge. Signing capacity contracts, where users pay based on the agreed contracted capacity, can help reduce electricity charges. It must be noted, however, that in order to reduce electricity costs, users must obtain a favourable tariff and carefully plan an appropriate contracted capacity [5,6]. Accurate peak demand prediction for different time periods is essential for setting an appropriate contract capacity. It plays a critical role for electricity users, enabling better decision-making in future planning. However, peak demand prediction is challenging due to the influence of various factors such as climate and seasonal variations [7]. Because the available data samples are often limited, risk assessment becomes valuable in providing some information to decision-makers [8,9]. For decision-makers, comprehensive risk assessments offer insights into the full distribution of potential outcomes, which supports more informed decision-making.

In recent decades, extensive research has been conducted in the field of electricity demand prediction [10]. A simplified method for forecasting Poland's long-term peak electricity demand using a modified Prigogine logistic equation was proposed [11]. Decomposition methodologies for identifying fluctuation characteristics in electricity demand forecasting were reviewed [12]. Turkey's current energy landscape was analyzed and long-term electricity demand forecasts were developed using a variety of statistical and machine learning models, including linear regression, polynomial regression, and artificial neural networks (ANNs) [13]. An optimal design for seasonal Time-of-Use tariffs was proposed based on the price elasticity of electricity demand [14]. An integrated approach combining artificial intelligence models, data augmentation techniques, and metaheuristic optimization algorithms to predict energy consumption one year in advance was employed. The models were trained and validated using historical energy consumption and weather data [15]. Recent technological advancements in energy management for university campuses were outlined, emphasizing their applicability to campus buildings and analyzing the roles of users [16]. A novel hybrid approach that combines classical statistical methods and machine learning to forecast national electricity demand was proposed [17]. A two-phase framework, which encompasses XGBoost-driven demand forecasting and PPO-guided dynamic pricing, specifically for Electric Vehicles (EV) charging stations, was also proposed. It provided particularly crucial information for real-time applications, where dynamic pricing is contingent upon exact short-term forecasts [18]. Foundational concepts within electricity and carbon markets were introduced and their advantages and limitations were analyzed in the context of EV participation in electricity markets [19]. A novel data-driven prediction model that fuses a multi-head self-attention (MHSA) mechanism and bi-directional long short-term memory (BiLSTM) to capture different types of dependencies from large-scale high-dimensional data was proposed [20]. A deep learning method (CNN-BiGRU-AM) that incorporates a convolutional neural network (CNN), bidirectional gated recurrent unit (BiGRU) and attention mechanism (AM) for fuel cell degradation prediction was also proposed. Accurate forecasting enables managers to better adapt to dynamic load changes and to formulate effective management strategies, providing a crucial basis for future electricity consumption planning and decision-making [21,22]. However, electricity demand forecasting is often challenged by the limited availability of historical data, in-

creasing the risk of inaccurate predictions. Risk plays a major role in this process [23,24]. Decision-makers require comprehensive risk assessments that provide a full distribution of potential outcomes before making informed decisions. To address this, the Enhanced Monte Carlo (EMC) method conducts a credibility-based risk assessment. It performs a comprehensive risk analysis through large-scale random sampling simulations. With extensive simulation testing, the EMC method produces more reliable and stable results, offering strong support for determining appropriate contract capacity.

This paper combines the advantages of the Grey Model (GM) [25] and Markov Chain [26] to propose a Grey–Markov Model (GMM) for predicting users' peak electricity demand across various periods. The study also proposed the Enhanced Monte Carlo (EMC) method to assess the credibility of electricity consumption predictions, providing risk analysis for users and helping decision-makers better understand consumption patterns and manage associated risks. A campus is used as a case study. Historical data on the monthly maximum electricity demand is collected to support the prediction, and a database is established using Microsoft Excel. The GMM is employed to predict the monthly maximum values of peak demand, semi-peak demand, Saturday semi-peak demand, and off-peak demand for a target year. The prediction results are then compared with those of the GM and the Grey Differential Equation (GDE) model [27] to evaluate efficiency and accuracy. Furthermore, the dual-variable method is integrated into the Monte Carlo simulation to propose the EMC model, which enhances the reliability of risk assessments. Simulation results demonstrate that this approach provides valuable references for future electricity consumption planning and risk management, as well as quality information for contract capacity setting [28].

2. Grey–Markov Model

The GMM is a Markov-chain-based search method built upon the GM. It is capable of handling nonlinear and non-stationary time series data and is especially effective for datasets with significant fluctuations or randomness. GMM enhances the accuracy of grey prediction by correcting residuals through the Markov chain. By introducing a state transition probability matrix, GMM not only captures the overall trend of the data but also adjusts local fluctuations, thereby demonstrating higher adaptability in complex data environments.

2.1. GM (1, 1) Model

Assume that the original data sequence is given in Equation (1).

$$X^0 = \left\{x^0(1), x^0(2), \ldots, x^0(n)\right\} \quad n \geq 4 \tag{1}$$

n is the number of original data, and $x^0(k)$ is the k-th data. The cumulative generation sequence $x^1(k)$ is shown in Equation (2).

$$x^1(k) = \left\{x^1(1), x^1(2), \ldots, x^1(n)\right\}, \quad x^1(k) = \sum_{i=1}^{k} x^0(i), k = 1, 2, \ldots, n \tag{2}$$

Assume that x^1 satisfies the first-order differential equation as shown in Equation (3).

$$\frac{dx^1}{dt} + ax^1 = b \tag{3}$$

a is the development coefficient of the grey prediction system, and b represents the external driving force. The equation is discretized based on differential equations, and its discrete form is shown in Equation (4).

$$x^0(k) + az^1(k) = b,\ k = 1, 2, 3, \ldots, n \tag{4}$$

$z^1(k)$ is the background value of x^1, which is calculated as Equation (5).

$$z^1(k) = \frac{1}{2}\Big(x^1(k) + x^1(k+1)\Big) \tag{5}$$

Equation (5) can be converted to matrix form as shown in Equation (6).

$$Y = ZB \tag{6}$$

$$Y = \begin{bmatrix} x^0(2) \\ x^0(3) \\ \vdots \\ x^0(n) \end{bmatrix},\ Z = \begin{bmatrix} -z^1(2) & 1 \\ -z^1(3) & 1 \\ \vdots & \vdots \\ -z^1(n) & 1 \end{bmatrix},\ B = \begin{bmatrix} a \\ b \end{bmatrix}$$

The least squares method is used to estimate the parameters $B = [a, b]^T$ as shown in Equation (7).

$$B = \Big(Z^T Z\Big)^{-1} Z^T Y \tag{7}$$

By solving the differential equation, the prediction function ($\hat{x}^1$) can be obtained as shown in Equation (8).

$$\hat{x}^1(k) = \left(x^1(0) - \frac{b}{a}\right)e^{-a(k-1)} + \frac{b}{a} \tag{8}$$

The accumulated data is restored to obtain the predicted value of the original data sequence as show in Equation (9).

$$\hat{x}^0(k) = (1 - e^{a\cdot})\left(x^0(1) - \frac{b}{a}\right)e^{-a(k-1)},\ \ k = 1, 2, 3, \ldots, n \tag{9}$$

The prediction value sequence generated by the GM (1, 1) is shown as Equation (10).

$$\hat{X}^0 = \Big\{\hat{x}^0(1), \hat{x}^0(2), \ldots, \hat{x}^0(n)\Big\} \tag{10}$$

For the residual sequence between the actual value and the predicted value is shown in Equations (11) and (12).

$$e(k) = x^0(k) - \hat{x}^0(k) \tag{11}$$

$$E = \{e(1), e(2), \ldots, e(n)\} \tag{12}$$

The GDE model is a variant of grey theory. It enhances the GM (1, 1) model by introducing a weighted background value in the accumulated generated sequence, thereby improving prediction accuracy. At its core, the GDE uses a first-order differential equation to describe the system's dynamic behaviour. The parameter α introduces a weighted background value $z^1(k)$, which is particularly suitable for handling data with exponential growth trends. Equation (5) is thus rewritten as Equation (13).

$$z^1(k) = \alpha x^1(k) + (1 - \alpha)x^1(k-1)\ \ \alpha \in [0, 1] \tag{13}$$

The key advantage of the GDE over GM (1, 1) is that the parameter α serves as an adjustable background value, offering greater flexibility and adaptability to the data. This enhances the model's robustness and prediction accuracy.

2.2. Markov Chain

In Markov Chain, the transition probability from state X_t to state X_{t+1} can be defined in Equation (14).

$$P_{ij} = P\{X_{t+1} = j | X_t = i\} \tag{14}$$

P_{ij} is the transition probability. $j = 0,\ 1.2.\ \ldots,\ n;\ i = 1,\ 1,\ 2,\ \ldots,\ n$. The transition matrix can be defined as Equation (15).

$$P_{ij}^{n} = \begin{bmatrix} p_{00} & p_{01} & p_{02} & \ldots.. & p_{0n} \\ p_{10} & p_{11} & p_{12} & \ldots.. & p_{1n} \\ & & . & & \\ & & . & & \\ p_{n0} & p_{n1} & p_{n2} & \ldots.. & p_{nn} \end{bmatrix} \tag{15}$$

By using Chapman–Kolmogorov equation [29], the prediction behaviour is shown in Equation (16)

$$P_{ij}^{n} = \sum_{k=1}^{s} P_{ik}^{m} P_{kj}^{n-m}\ \forall i, j;\ 0 < m < n \tag{16}$$

2.3. Grey–Markov Model

GM (1, 1) is used to reveal the development and change trends of the predicted series, while the Markov model determines the state transition rules. The GMM combines the Markov chain with GM (1, 1) to handle nonlinear and non-stationary time series data. It is particularly suitable for datasets with large fluctuations or randomness. By introducing the Markov chain to correct residuals, GMM improves the accuracy of grey prediction. It not only captures the overall trend but also adjusts local fluctuations through the state transition probability matrix, thereby demonstrating greater resilience in complex data environments. The procedure of GMM is described as follows.

Step 1. Division of Status

The research period divided into ω status, where $\hat{x}^0(k)$ is the centre point of ω status as shown in Equation (17). Each actual value must belong to the status, and the upper and lower bounds of ω status are defined as Equations (18) and (19).

$$S_{ki} \in [L_{ki}, U_{ki}],\ i = \mathrm{i}, 2, \ldots, \omega \tag{17}$$

$$U_{ki} = \hat{x}^0(k)(1 + 0.5R) \tag{18}$$

$$L_{ki} = \hat{x}^0(k)(1 - 0.5R) \tag{19}$$

U_{ki} and L_{ki} are the upper and lower bounds of status i in period k. R is the parameter of status, which is defined by users.

Step 2. Calculate the state transition matrix

M_{ij}^{t} is the number of times status i transitions to status j via seep t. The probability of status i transitioning to status j via seep t is express as Equation (20).

$$P_{ij}^{t} = \frac{M_{ij}^{t}}{M_i}\ \ j = 1, 2,\ \ldots, \omega \tag{20}$$

M_i is the number of status i. The GMM transition probability matrix can be express in Equation (21).

$$P_{ij}^t = \begin{bmatrix} P_{11}^t & P_{12}^t \ldots\ldots P_{1\omega}^t \\ P_{21}^t & P_{22}^t \ldots\ldots P_{2\omega}^t \\ & \cdot \\ & \cdot \\ & \cdot \\ P_{\omega 1}^t & P_{\omega 2}^t \ldots\ldots P_{\omega\omega}^t \end{bmatrix} \tag{21}$$

Step 3. Determine the predicting value

After determining the transition status, it can predict the possible status of k-th period. The interval structure of this status is $S_{k+1,j} \in \left[L_{k+1,j}, U_{k+1,j}\right]$. The k-th prediction value $\hat{x}_{k+1}$ is the middle point of the upper and lower bounds of the status interval as shown in Equation (22).

$$\hat{x}_{k+1} = \frac{1}{2}\left(L_{k+1,j} + U_{k+1,\,j}\right) \tag{22}$$

Step 4. Evaluation of predicting accuracy

This paper uses the Mean Absolute Percentage Error (MAPE) to test the credibility of the predicted value for the evaluation of prediction accuracy as shown in Equations (23) and (24).

$$error = \frac{\left|x^0(k) - \hat{x}^0(k)\right|}{x^0(k)} \times 100\% \tag{23}$$

$$MAPE = \frac{1}{n}\sum_{k=1}^{n} \frac{\left|x^0(k) - \hat{x}^0(k)\right|}{x^0(k)} \times 100\% \tag{24}$$

$x^0(k)$ is the actual value of the k-th period. $\hat{x}^0(k)$ is the predicted value of the k-th period. The prediction ability evaluation of MAPE is shown in Table 1 [29].

Table 1. The prediction ability evaluation of MAPE.

MAPE Value	**<10%**	**10%~20%**	**20%~50%**	**>50%**
prediction ability	High accuracy	Good	Reasonable	Inaccuracy

3. Enhanced Monte Carlo

Monte Carlo (MC) [30] is a risk assessment tool primarily used to simulate the distribution of random events and evaluate their associated risks or uncertainties. The Enhanced Monte Carlo (EMC) method employs dual variables to offset positive and negative deviations, thereby reducing estimation errors. Specifically, EMC introduces pairs of negatively correlated random variables to decrease simulation error in MC. By incorporating error reduction techniques, dynamic data updates, and the ability to handle complex scenarios, EMC enhances the performance of MC and provides a more scientific and comprehensive approach to risk assessment.

In the MC, the estimator ($\hat{\theta}$) of probability density function is calculated as shown in Equation (25).

$$\hat{\theta} = \frac{1}{N}\sum_{i=1}^{N} f(X_i) \tag{25}$$

$f(X_i)$ is the probability density function. The dual-variable method introduces a paired sample to the probability density function, that is, $f_X(X_i) = f_X(-X_i)$, which X_i and $-X_i$ shares the same probability density function. The dual function can be expressed as shown in Equation (26).

$$Y_i = f(X_i) \text{ and } \widetilde{Y}_i = f(-X_i) \tag{26}$$

Since X_i and $-X_i$ are symmetric and have the same expected value. The dual-variable method defines the dual variables by generating n independent and identically distributed samples (X_1, X_2,..., X_n). For each sample X_i, its dual sample $-X_i$ is generated, and the values $Y_i = f(X_i)$ and $\widetilde{Y}_i = f(-X_i)$ are calculated. A new estimator is constructed by taking the mean of these dual variables. Since Y_i and $\widetilde{Y}_i$ share the same expected value, a new estimator Z_i can be defined as shown in Equation (27).

$$Z_i = \frac{Y_i + \widetilde{Y}_i}{2} \tag{27}$$

The expected value of the estimator $E[Z_i]$ is described as shown in Equation (28).

$$E[Z_i] = E\left[\frac{f(X_i) + f(-X_i)}{2}\right] = \theta \tag{28}$$

θ is an unpredictable value, which is simulated by covariance analysis to analyze the error of Z_i as shown in Equation (29).

$$\begin{aligned} \mathrm{Var}(Z_i) &= \mathrm{Var}\left(\tfrac{Y_i + \widetilde{Y}_i}{2}\right) \\ &= \tfrac{1}{4}\left[\mathrm{Var}(Y_i) + \mathrm{Var}\left(\widetilde{Y}_i\right) + 2\mathrm{Cov}\left(Y_i, \widetilde{Y}_i\right)\right] \\ &= \tfrac{1}{4}\left[2\mathrm{Var}(Y_i) + 2\mathrm{Cov}\left(Y_i, \widetilde{Y}_i\right)\right] \\ &= \tfrac{1}{2}\left[\mathrm{Var}(Y_i) + \mathrm{Cov}\left(Y_i, \widetilde{Y}_i\right)\right] \end{aligned} \tag{29}$$

If Y_i and $\widetilde{Y}_i$ are negatively correlated, that is, $\mathrm{Cov}\left(Y_i, \widetilde{Y}_i\right) < 0$, then $\mathrm{Var}(Z_i) < \mathrm{Var}(Y_i)$, thereby reducing the error. The most effective case of the dual-variable method is when $f(X_i)$ is a monotonic function. $f(X_i)$ is a linear function, as shown in Equations (30)–(32).

$$Y_i = f(X_i) = aX_i + b \tag{30}$$

$$\widetilde{Y}_i = f(-X_i) = -aX_i + b \tag{31}$$

$$Z_i = \frac{Y_i + \widetilde{Y}_i}{2} = b \tag{32}$$

In this case, the error of Z_i is 0, and the dual-variable method completely eliminates the error. The final estimator and average Z_i can be calculated as shown in Equation (33).

$$\hat{\theta}_{AV} = \frac{1}{N}\sum_{i=1}^{N} Z_i \tag{33}$$

The error of the estimator is smaller than that of the traditional MC method. The dual-variable method significantly reduces the simulation error by introducing negatively correlated paired samples. This approach is particularly effective when the objective function is monotonic or nearly linear. In such cases, the dual-variable method can substantially reduce the number of samples required, thereby improving computational efficiency.

In risk assessments, this paper primarily uses risk credibility as a key indicator, which significantly influences the results of risk assessment and decision analysis. Credibility refers to the reliability and accuracy of the risk assessment outcomes, reflecting the likelihood that the assessment results correspond to the actual situation. Higher credibility indicates more reliable assessment results. Decision makers can formulate risk management

strategies with greater confidence based on these results [31,32]. In this paper, credibility levels of 90% and 95% are employed, meaning there is a 90% or 95% confidence level that the assessment results are accurate. An increase in credibility from 90% to 95% implies greater reliability of the assessment results, thereby providing a more solid basis for decision-making.

4. Case Study

This paper collected the data from the EMS of Cheng-Shiu University. The monthly maximum electricity demand from 2018 to 2022 serves as the reference dataset for electricity demand prediction. The electricity demand data were collected from the Energy Management System (EMS) of Cheng-Shiu University [33]. High-voltage users adopt the Time-of-Use (TOU) rate structure, which is categorized into two-stage and three-stage types, as shown in Table 2 [4]. The GM, GDE, and GMM were applied to predict electricity demand, and the predicted results were then compared with the actual electricity demand in 2023. The error values were calculated and analyzed using the MAPE from Equation (24) to evaluate the effectiveness of the proposed method for users.

Table 2. The TOU rate structure of high voltage users.

Type	Demand Charge (NT$/KW)	
	Summer Month	Non-Summer Month
Peak contract	236.2	173.2
Semi-peak contract	173.2	173.2
Saturday Semi-peak contract	47.2	34.6
Off-peak contract	47.2	34.6

4.1. Demand Consumption Prediction

Table 3 presents the prediction results and error values of peak demand from May to October. For the GM, the MAPE is 10.46258%, with the highest prediction error of 13.23165% observed in May and the lowest error of 7.4995% in October. The GDE model achieves a lower MAPE of 9.414556%, where the maximum error occurs in June at 11.1649%, and the minimum error in October at 7.35202%. The proposed GMM outperforms both methods, yielding the lowest MAPE of 7.837098%. For GMM, the maximum error is recorded in September at 10.4334%, while the minimum error is achieved in October at 5.32796%. These results demonstrate that the GMM provides more accurate and stable predictions compared with the GM and GDE models.

Table 3. The prediction results and error values of peak demand consumption.

2023	GM		GDE		GMM	
Month	Prediction value (kW)	error (%)	Prediction value (kW)	error (%)	Prediction value (kW)	error (%)
1	0	0	0	0	0	0
2	0	0	0	0	0	0
3	0	0	0	0	0	0
4	0	0	0	0	0	0
5	3028.52	13.2316	3150.65	9.73255	3286.6	5.83752
6	2896.56	12.0482	2925.65	11.1649	2969.54	9.83224
7	2399.15	11.2724	2456.23	9.16141	2463.13	8.90623

Table 3. *Cont.*

2023	GM		GDE		GMM	
8	2501.23	10.4234	2564.23	8.16716	2605.61	6.68522
9	3179.71	8.2999	3089.23	10.9093	3105.73	10.4334
10	3214.09	7.49995	3219.23	7.35202	3289.56	5.32796
11	0	0	0	0	0	0
12	0	0	0	0	0	0
MAPE		10.46258		9.414556		7.837098

Table 4 presents the prediction results and error values of semi-peak demand consumption. The GM achieves a MAPE of 10.16044%, with the highest error of 14.93276% in February and the lowest error of 5.293361% in October. The GDE model performs slightly better, yielding a MAPE of 9.528247%. Its maximum error occurs in November (14.35687%), while the minimum is in March (1.945928%). In contrast, the proposed GMM attains the best overall accuracy, with the lowest MAPE of 4.978714%. For GMM, the maximum prediction error is 8.87251% in May, and the minimum error is 1.383277% in December. Overall, the GMM consistently outperforms both GM and GDE, producing lower errors and demonstrating superior predictive performance.

Table 4. The prediction results and error values of semi-peak demand consumption.

2023	GM		GDE		GMM	
Month	Prediction value (kW)	error (%)	Prediction value (kW)	error (%)	Prediction value (kW)	error (%)
1	2165.56	9.492285	2180.53	8.866627	2523.4	5.46333
2	1986.32	14.93276	2001.52	14.2818	2450.23	4.934904
3	2406.36	8.058045	2566.33	1.945928	2777.45	6.120523
4	2818.63	8.610364	3015.14	2.238837	3278.95	6.314786
5	3985.32	8.746574	3828.26	12.34284	3979.82	8.87251
6	3659.25	11.20071	3578.1	13.16998	3896.56	5.441891
7	2875.63	15.00567	2898.52	14.32912	3169.86	6.309187
8	2665.5	10.96719	2660.2	11.14422	3038.69	1.498076
9	3896.36	10.19563	3986.32	8.122211	4031.97	7.070058
10	4117.57	5.293361	4190.22	3.622367	4268.23	1.828089
11	2694.56	12.8431	2647.76	14.35687	3230.99	4.507993
12	2811.61	6.579546	2711.13	9.918163	3051.26	1.383227
MAPE		10.16044		9.528247		4.978714

Table 5 presents the prediction results and error values of Saturday semi-peak electricity consumption. The GM yields a mean absolute percentage error (MAPE) of 11.54289%, with the maximum error of 14.9468% occurring in May and the minimum error of 3.65114% in July. The GDE model performs better than GM, achieving a MAPE of 9.7707%. Its maximum prediction error is 18.6991% in March, while the minimum is 3.57968% in January. The proposed GMM attains the lowest MAPE of 5.053946%, with the maximum error of 10.3659% in November and the minimum of 0.44852% in February. Overall, the

GMM outperforms both GM and GDE, providing the most accurate predictions of Saturday semi-peak demand consumption throughout 2023.

Table 5. The prediction results and error values of Saturday semi-peak electricity consumption.

2023	**GM**		**GDE**		**GMM**	
Month	Prediction value (kW)	error (%)	Prediction value (kW)	error (%)	Prediction value (kW)	error (%)
1	1589.36	12.2612	1466.45	3.57968	1522.34	7.52735
2	1051.73	7.14103	993.56	12.277	1127.53	0.44852
3	1635.36	12.454	1518.7	18.6991	1789.56	4.19914
4	1791.61	14.433	1896.36	9.43018	2201.45	5.14087
5	2098.56	14.9468	2159.42	12.4802	2650.37	7.41767
6	2275.3	13.6404	2387.44	9.38406	2616.25	0.69952
7	2242.14	3.65114	2070.85	4.26737	2249.27	3.98075
8	1720.56	10.1132	1783.19	6.84119	2046.59	6.91956
9	2539.65	8.44809	2673.12	3.63663	2837.77	2.29885
10	2478.55	10.8355	2453.15	11.7493	2972.46	6.93264
11	2045.56	17.294	2189.56	11.4718	2729.67	10.3659
12	2087.56	13.2965	2084.48	13.4244	2521.26	4.71653
MAPE		11.54289		9.77007		5.053946

Table 6 shows the prediction results and error values of off-peak demand consumption. The MAPE of the GM is 11.68772%. The maximum prediction error occurs is 15.9136% in July, and the minimum occurs is 5.12231%in January. The MAPE of the GDE is 8.619784%, which is slightly better than the GM. The maximum prediction error is 13.1232% in July, and the minimum is 4.74284% in January. The MAPE of the GMM proposed in this paper is 6.794887%, which is the lowest average error among the three methods. The maximum prediction error is 9.53771% in September, and the minimum is 3.57934% in January. The GMM performs better than the other two methods in predicting off-peak demand consumption from January to December 2023.

Table 6. The prediction results and error values of off-peak demand consumption.

2023	**GM**		**GDE**		**GMM**	
Month	Prediction value (kW)	error (%)	Prediction value (kW)	error (%)	Prediction value (kW)	error (%)
1	907.6	5.12231	911.23	4.74284	922.36	3.57934
2	1356.25	14.0363	1398.56	11.3545	1456.25	7.69791
3	1580.58	10.6219	1602.35	9.39087	1632.58	7.68143
4	1836.82	11.8570	1869.45	10.2912	1898.72	8.88666
5	2145.36	9.03131	2204.35	6.52999	2245.78	4.77325
6	1986.25	10.7400	2047.36	7.99374	2089.56	6.09732
7	1536.25	15.9136	1587.23	13.1232	1701.05	6.89331
8	1425.68	11.8138	1523.12	5.78659	1473.6	8.84967

Table 6. *Cont.*

2023	GM		GDE		GMM	
9	1989.56	15.0817	2145.89	8.4092	2119.45	9.53771
10	2019.58	13.9784	2133.41	9.12998	2215.26	5.64368
11	1869.56	10.5015	1967.49	5.8135	1979.08	5.25867
12	1798.56	11.5548	1812.45	10.8717	1898.51	6.63969
MAPE		11.68772		8.619784		6.794887

Table 7 shows the prediction errors of demand consumption. The maximum MAPE in the GM is 11.68772%, which occurs during the off-peak period. The maximum in the GDE is 9.77007%, observed during the Saturday off-peak period. For the GMM, the maximum error is 9.414556%, occurring during the peak period. The average MAPE of the GM is the highest among the three methods, at 10.96341%. The average MAPE of the GDE is 9.333164%, which is slightly better than that of the GM. The GMM has the smallest average MAPE, at 6.560526%. Due to demand consumption often exhibits multi-peak and mutation characteristics, the fitting ability of the GMM lead to increased prediction deviations and the errors are quite large. According to Table 1, the evaluation of prediction ability shows that both GDE and GMM achieve the high accuracy, with GMM performing the best. The proposed GMM demonstrates strong predictive ability and has significant reference value. Overall, the results clearly indicate that the proposed GMM provides the most accurate and reliable predictions across different electricity demand conditions, making it a more effective tool for forecasting than GM and GDE. GMM is highly sensitive to initial values. If there are measurement errors in the initial data, it will cause continuous deviations in the cumulative generated sequence, resulting in systematic errors in the model output. In addition, the transition matrix needs to be frequently reconstructed due to the data fluctuation, otherwise the prediction accuracy will decrease. The results highlight the strong predictive capability of the GMM and confirm the strongest performance.

Table 7. The prediction errors of the demand consumption.

	GM	GDE	GMM
The MAPE of peak demand (%)	10.46258	9.414556	7.837098
The MAPE of semi-peak demand (%)	10.16044	9.528247	4.978714
The MAPE of Saturday semi-peak demand (%)	11.54289	9.77007	5.053946
The MAPE of off-peak demand (%)	11.68772	8.619784	6.794887
Average MAPE (%)	10.96341	9.333164	6.560526

4.2. Risk Assessment of Demand Consumption

Peak demand consumption, semi-peak demand consumption, Saturday semi-peak demand consumption, and off-peak demand consumption are the four most important categories. Among them, the prediction error of peak demand consumption directly affects the setting of contract capacity. This paper uses the GMM to predict peak demand consumption in order to evaluate the impact of electricity demand uncertainty, and applies the EMC method to assess and analyze the associated risk, providing decision-makers with a more comprehensive understanding of demand variability and its implications for energy management.

Table 8 presents 10,000 risk assessment results for peak demand prediction at confidence levels of 90% and 95%. Risk probability reflects the degree of variation in the data across the target year. A greater error difference corresponds to a higher risk probability. It

can be seen that the month with the highest variation in values across the years is May. The peak demand prediction errors in May are 16.57% at 90% confidence and 10.37% at 95% confidence, representing the highest prediction error. In contrast, June has the lowest variation, with prediction errors of 1.83% and 0.95% at the 90% and 95% confidence levels, respectively, the lowest among all months. Using the GMM-based risk assessment, the MAPE is reduced to 9.31% at 90% confidence and further reduced to 5.37% at 95% confidence.

Table 8. The risk evaluation of peak demand consumption prediction.

2023		Risk Probability (%)	90% Confidence Level		95% Confidence Level	
Month	Actual Value (kW)		Risk Margin (kW)	Error (%)	Risk Margin (kW)	Error (%)
1	0	0	0	0	0	0
2	0	0	0	0	0	0
3	0	0	0	0	0	0
4	0	0	0	0	0	0
5	3490.35	24.38	2955.12	16.57	3155.16	10.37
6	3293.35	2.39	3234.08	1.83	3324.03	0.95
7	2703.95	22.42	2278.40	13.17	2380.52	10.01
8	2792.28	7.08	2463.51	10.18	2686.44	3.28
9	3467.51	2.83	3357.25	3.41	3528.93	1.90
10	3474.69	12.74	3128.89	10.70	3290.92	5.69
11	0	0	0	0	0	0
12	0	0	0	0	0	0
MAPE		11.97		9.31		5.37

Figure 1 shows the EMC risk assessment for May. The distribution of 10,000 simulated data points is displayed. The risk assessment value is calculated to be 2955.12 kW at a 90% confidence level, and 3155.16 kW at a 95% confidence level. These results highlight that higher confidence levels are associated with greater assessed demand, reflecting the increased allowance for prediction error under higher risk probabilities. This analysis demonstrates the capability of the EMC method to quantify the uncertainty in electricity demand forecasting and to provide decision-makers with a probabilistic framework for risk-informed planning.

Figure 2 shows the EMC risk assessment for June. The distribution of 10,000 simulated data points is presented. The risk assessment value is calculated as 3234.08 kW at a 90% confidence level and 3324.03 kW at a 95% confidence level. These results indicate that lower risk probabilities correspond to smaller prediction errors, while higher confidence levels require accounting for greater uncertainty in demand. This demonstrates the effectiveness of the EMC in quantifying forecast uncertainty and supporting risk-informed decision-making in electricity demand management.

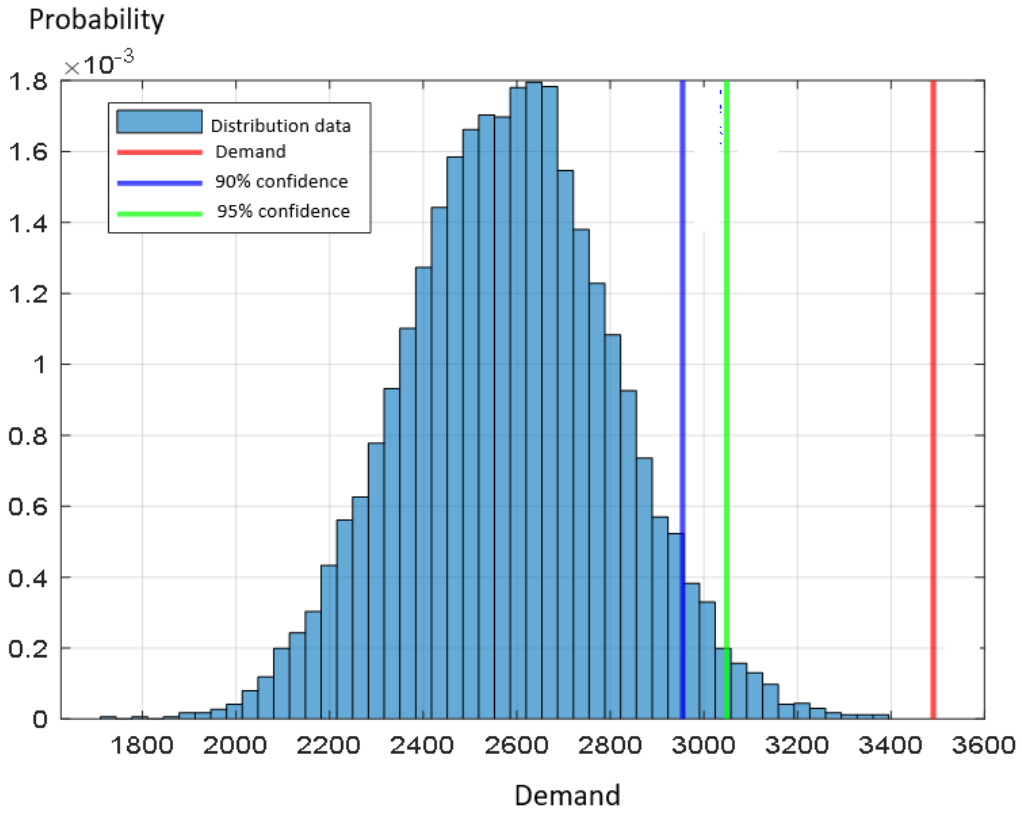


Figure 1. The risk assessment of EMC in May.

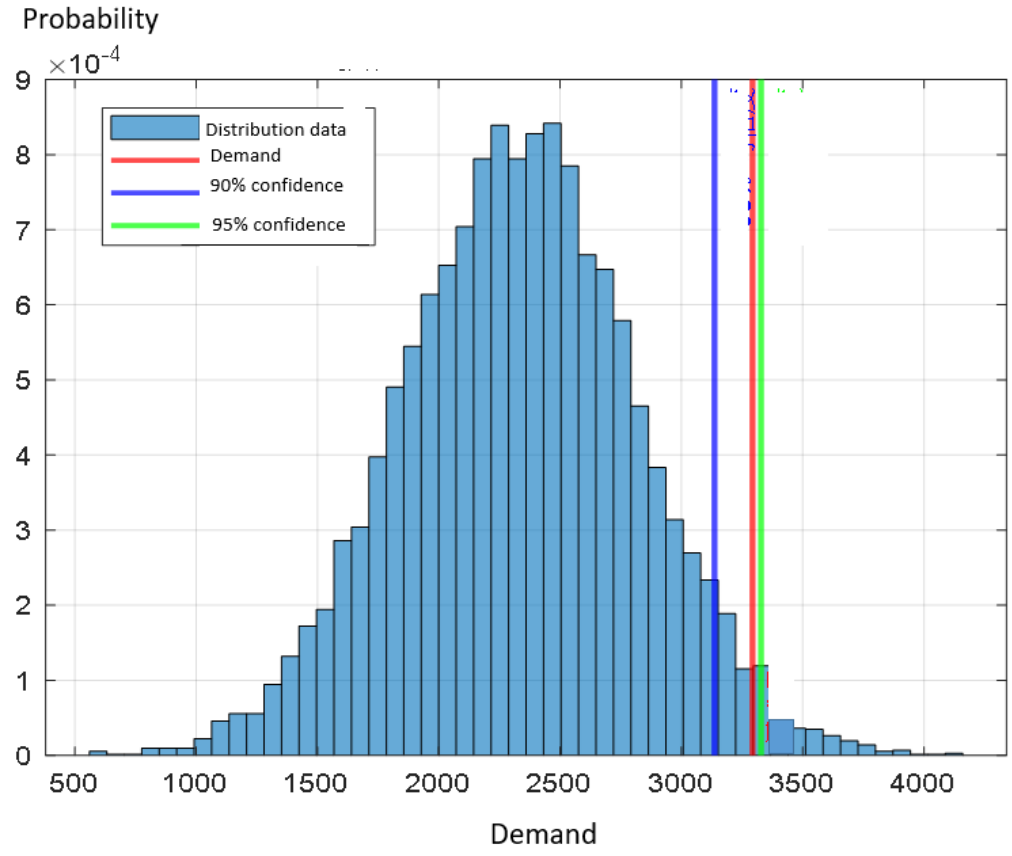


Figure 2. The risk assessment of the EMC in June.

5. Conclusions

This paper proposes an improved method for grey theory by incorporating Markov chain analysis, resulting in the Grey–Markov Model (GMM). The GMM addresses the limitations of traditional grey prediction models, which require large amounts of data and struggle with incomplete or unreliable historical data. By leveraging Markov chains, the GMM effectively handles sequential data and captures the transition probabilities between data points. Furthermore, when dealing with data exhibiting both trends and fluctuations, the GMM generates predictions using the grey prediction model and then refines these predictions using the Markov chain, thus achieving more accurate results. This paper also employs the EMC method to perform a credibility risk assessment on demand consumption predictions. For risk assessment, a large number of random sampling simulations are conducted to provide a comprehensive risk analysis, helping decision-makers better understand and manage risks. Additionally, through extensive simulation testing, more reliable and stable results can be obtained, offering strong support for contract capacity setting. The findings of this paper are not only applicable to university campuses but can also be extended to the power management systems of other industrial areas. By applying the Grey–Markov Model (GMM) and Enhanced Monte Carlo (EMC) methods, these facilities can achieve more accurate electricity demand forecasting and risk assessment, leading to optimized contract capacity agreements, reduced electricity costs, and improved energy efficiency. Furthermore, enhanced prediction accuracy allows for dynamic monitoring of power operation strategies, enabling more precise and efficient energy management.

6. Discussion

While the proposed method demonstrates excellent performance in theoretical and case studies, some technical challenges remain for its practical application. Although the GMM has low requirements for historical data, its prediction accuracy may be affected when dealing with extreme weather or unexpected events. Future research could consider incorporating more external variables, such as weather forecasts or holiday schedules, to enhance the adaptability of the GMM. While the EMC provides comprehensive risk assessment, its high computational complexity, especially when processing large datasets, may lead to insufficient computational resources. This paper offers new insights and methods for campus energy management. With continuous improvement and system expansion, it holds promise for achieving accurate and intelligent energy management in broader applications.

Author Contributions: M.-T.T. generalizes novel algorithms and designs system planning projects and prepared the manuscript as the corresponding author. Y.-H.T. is the first author. He conducted the theory experiments and simulation tool and performed the formal analysis and data investigation. All the authors were involved in exploring system validation and the results, as well as permitting the benefits of the published document. All authors have read and agreed to the published version of the manuscript.

Funding: This research received no external funding.

Data Availability Statement: The original contributions presented in this study are included in the article. Further inquiries can be directed to the corresponding author.

Acknowledgments: We would like to thank the Cheng-Shiu University, Taiwan for financial support. (Grant Nos. D-2-2-1 Promotion of Industry–Academia New Technology Research Projects).

Conflicts of Interest: The authors declare no conflicts of interest.

Abbreviations

The following abbreviations are used in this manuscript:

ANN	Artificial Neural Network
EMC	Enhanced Monte Carlo
EMS	Energy Management System
EV	Electric Vehicles
GDE	Grey Differential Equation
GM	Grey Model
GMM	Grey–Markov Model
MC	Monte Carlo
TOU	Time-of-Use

References

1. Chen, M.; Xie, Z.; Sun, Y.; Zheng, S. The predictive management in campus heating system based on deep reinforcement learning and probabilistic heat demands forecasting. *Appl. Energy* **2023**, *350*, 121710. [CrossRef]
2. Alsamraee, S.A.; Khanna, S. High-resolution energy consumption forecasting of a university campus power plant based on advanced machine learning techniques. *Energy Strategy Rev.* **2025**, *60*, 101769. [CrossRef]
3. Zhakiyev, N.; Satan, A.; Akhmetkanova, G.; Medeshova, A.; Omirgaliyev, R.; Bracco, S. Energy Management System for the Campus Microgrid Using an Internet of Things as a Service (IoTaaS) with Day-ahead Forecasting. *Procedia Comput. Sci.* **2024**, *241*, 488–493. [CrossRef]
4. Taiwan Power Company. The Electricity Tariff Structure of TPC. Available online: http://taipower.com.tw/tc/indexaspx (accessed on 1 July 2024).
5. Fernandez, M.A.; Zorita, A.L.; Escudero, L.A.; Duque, O.; Morinigo, D.; Riesco, M. Cost optimization of electrical contracted capacity for large customers. *Int. Electr. Power Energy Syst.* **2013**, *46*, 123–131. [CrossRef]
6. Yang, S.H. Demand Forecasting Method Based Contract Capacity Optimization. Master's Thesis, National Cheng Kung University, Tainan, Taiwan, 2013.
7. Falasca, S.; Zinzi, M.; Siani, A.M.; Curci, G.; Ding, L.; Santamouris, M. Investigating the effects of the greenery increase on air temperature, ventilation and cooling energy demand in Melbourne with the Weather Research and Forecasting model and Local Climate Zones. *Sci. Total Environ.* **2024**, *953*, 176016. [CrossRef] [PubMed]
8. Hansen, T.V.A.; Nielsen, J.P. Risk-based sampling for surveillance of medicinal residues in carcasses of pigs and cattle: A scoping review. *Prev. Vet. Med.* **2025**, *243*, 106602. [CrossRef] [PubMed]
9. Chen, Y.; Wang, Y.; Headley, J.V.; Huang, R. Sample preparation, analytical characterization, monitoring, risk assessment and treatment of naphthenic acids in industrial wastewater and surrounding water impacted by unconventional petroleum production. *Sci. Total Environ.* **2024**, *913*, 169636. [CrossRef]
10. Popławski, T. Long-Term Forecast of Peak Power Demand for Poland—Construction and Use of Simplified Forecasting Models. *Energies* **2025**, *18*, 3472. [CrossRef]
11. Shao, Z.; Fu, C.; Yang, S.L.; Zhou, K.L. A review of the decomposition methodology for extracting and identifying the fluctuation characteristics in electricity demand forecasting. *Renew. Sustain. Energy Rev.* **2017**, *75*, 123–136. [CrossRef]
12. Köse, E.; Kaynar, S.K. Energy Demand Forecasting and Policy Development in Turkey. *Energies* **2025**, *18*, 3301. [CrossRef]
13. Mu, Y.; Tan, H.; Jia, Y.; Wang, X.; Zhao, H.; Zhao, Y. Research on the Optimal Design of Seasonal Time-of-Use Tariff Based on the Price Elasticity of Electricity Demand. *Energies* **2023**, *16*, 1625. [CrossRef]
14. Chou, J.H.; Nguyen, H.M. Simulating long-term energy consumption prediction in campus buildings through enhanced data augmentation and metaheuristic-optimized artificial intelligence. *Energy Build.* **2024**, *312*, 114191. [CrossRef]
15. Kolokotsa, D.; Yang, J.; Eang, L. Energy management in university campuses. *Ref. Modul. Earth Syst. Environ. Sci.* **2025**, *9*, 614–632. [CrossRef]
16. Grandón, A.T.G.; Schwenzer, J.; Steens, T.; Breuing, J. Electricity demand forecasting with hybrid classical statistical and machine learning algorithms: Case study of Ukraine. *Appl. Energy* **2024**, *355*, 122249. [CrossRef]
17. Mahmud, M.; Abedin, T.; Rahman, M.; Shoishob, S.A.; Kiong, T.S.; Nur-E-Alam, M. Integrating demand forecasting and deep reinforcement learning for real-time electric vehicle charging price optimization. *Util. Policy* **2025**, *96*, 102038. [CrossRef]
18. Lei, X.; Zhong, J.; Chen, Y.; Shao, Z.; Jian, L. Grid integration of electric vehicles within electricity and carbon markets: A comprehensive overview. *eTransportation* **2025**, *25*, 100435. [CrossRef]
19. Jia, C.; He, H.; Zhou, J.; Li, K.; Li, J.; Wei, Z. A performance degradation prediction model for PEMFC based on bi-directional long short-term memory and multi-head self-attention mechanism. *Int. J. Hydrogen Energy* **2024**, *60*, 133–146. [CrossRef]

20. Zhou, J.; Shu, X.; Zhang, J.; Yi, F.; Jia, C.; Zhang, C.; Kong, X.; Zhang, J.; Wu, G. A deep learning method based on CNN-BiGRU and attention mechanism for proton exchange membrane fuel cell performance degradation prediction. *Int. J. Hydrogen Energy* **2024**, *94*, 394–405. [CrossRef]
21. Dong, X.; Guo, W.; Zhou, C.; Luo, Y.; Tian, Z.; Zhang, L.; Wu, X.; Liu, B. Hybrid model for robust and accurate forecasting building electricity demand combining physical and data-driven methods. *Energy* **2024**, *311*, 133309. [CrossRef]
22. Al-Abri, A.; Okedu, K. Overview of the Global Electricity System in Oman Considering Energy Demand Model Forecast. *Energy Eng.* **2022**, *120*, 409–423. [CrossRef]
23. Zhang, X.; Zhang, D.; Zhou, Y.; Hua, K. Energy Risks Zoning and Demand Forecasting in Jiangsu rovince. *Energy Procedia* **2011**, *5*, 813–817. [CrossRef]
24. Choi, T.M.; Ren, S. Intelligent demand forecasting supported risk management systems for fast fashion inventory management. In *Information Systems for the Fashion and Apparel Industry*; Woodhead Publishing: Cambridge, UK, 2016; pp. 263–271. [CrossRef]
25. Jiang, J.; Zhang, M.; Huang, Z. A new adaptive grey prediction model and its application. *Alex. Eng. J.* **2025**, *120*, 515–522. [CrossRef]
26. Tjakra, J.; Bao, J.; Hudon, N.; Yang, R. Modeling collective dynamics of particulate systems under time-varying operating conditions based on Markov chains. *Adv. Powder Technol.* **2013**, *24*, 451–458. [CrossRef]
27. Zhang, F.; Xiao, X.; Gao, M. An extended neural ordinary differential equation network with grey system and its applications. *Neurocomputing* **2024**, *576*, 127343. [CrossRef]
28. Tsay, M.T.; Lin, W.M.; Lee, J.L. Optimal contracts decision of industrial customers. *Int. J. Electr. Power Energy Syst.* **2001**, *23*, 795–803. [CrossRef]
29. Aluigi, A.; Corradini, M.; Gheno, A. Chapman–Kolmogorov lattice method for derivatives pricing. *Appl. Math. Comput.* **2014**, *226*, 606–614. [CrossRef]
30. Caralis, G.; Diakoulaki, D.; Yang, P.; Gao, Z.; Zervos, A.; Rados, K. Profitability of wind energy investments in China using a Monte Carlo approach for the treatment of uncertainties. *Renew. Sustain. Energy Rev.* **2014**, *40*, 224–236. [CrossRef]
31. Antonio, C. *Risk Management Tools and Analysis*; John Wiley & Sons Ltd.: Hoboken, NJ, USA, 2012. [CrossRef]
32. Marrison, C. *Fundamentals of Risk Measurement*; McGraw-Hill Companies, Inc.: Chicago, IL, USA, 2002.
33. Energy Management System of Cheng-Shiu University. Available online: http://120.118.246.40:8080/ECOA/index.jsp (accessed on 2 July 2024).

Disclaimer/Publisher's Note: The statements, opinions and data contained in all publications are solely those of the individual author(s) and contributor(s) and not of MDPI and/or the editor(s). MDPI and/or the editor(s) disclaim responsibility for any injury to people or property resulting from any ideas, methods, instructions or products referred to in the content.